

## Weyl-Heisenberg and Wavelet Coherent Frames for SAR Ocean Image Filtering

J. G. Teti, Jr.  
Microwave Technology Division  
Naval Air Warfare Center, Aircraft Division  
Warminster, PA 18974

H. N. Kritikos  
Moore School of Electrical Engineering  
University of Pennsylvania  
Philadelphia, PA 19104

**Abstract** - Filtering SAR imagery for the purposes of speckle reduction, and feature or information extraction is a re-occurring subject area in microwave remote sensing. Existing classical techniques such as pixel averaging, median filtering, pyramidal filtering, etc., are often accompanied by troubling performance tradeoffs depending on the application. In this work a novel filtering method based on coherent frame theory is described and exercised on a SAR ship wake image. The method is demonstrated to be a unique and potentially powerful analytical tool for SAR image analysis. Two different types of coherent frames are studied related to applications of the Weyl-Heisenberg and affine or wavelet groups used in quantum physics to describe atomic coherent states. In both cases the particular coherent frames selected consist of frame elements having simultaneous localization in phase space which satisfies the lower limit of the uncertainty principle. Using frames of this type are ideal for the representation of waveforms which arise from nonstationary processes.

### Introduction

There are a number of approaches that may be taken to extract information directly from SAR ocean imagery. In this paper we first decompose the SAR ocean image in terms of "fundamental" elements, and then perform a limited reconstruction that results in a filtered image. Since the SAR ocean image is formed from data originating from a nonstationary scene (process), it is desirable to decompose the image into fundamental elements which have optimum simultaneous localization (OSL) in phase space. Note that the term "optimum" is used in the sense that the lower limit of the uncertainty principle is satisfied, and phase space is the two dimensional space-wavenumber or time-frequency space. It is well known that if a waveform is to have the OSL property it must be based on a Gaussian function. The decomposition and reconstruction of an image in terms of fundamental elements of this type present some serious numerical difficulties because the elements are cross coupled. The cross coupling can be handled with use of coherent frame concepts. Daubechies was the first to recognize the usefulness of frame concepts and used them to unify both a Weyl-Heisenberg and affine or wavelet type of discrete localized time-frequency analysis [1]. In general, a Weyl-Heisenberg frame consists of frame elements that are related by translation and modulation, and the wavelet frame consists of frame elements which are related by translation and dilation. Both frames can be generated by a single "mother" function. The OSL property in the Weyl-Heisenberg case leads to the use of the Gabor transform, and was investigated in [2]. The affine case uses the wavelet transform with a modulated Gaussian wavelet as its mother function and was investigated in [3]. Our earlier work discussed the potential application of these frame representations for filtering and here we exercise a specific filtering algorithm. A very brief discussion of the relevant theory is also included.

### Theory and Computational Procedure

Each frame allows the exact representation of waveforms  $f$  which are members of the Hilbert space  $\mathcal{H}$  spanned by the frame. Note that a frame is generally not a basis for the space it spans, since when

expressed in the form of a complete irreducible set, the number of frame elements may be larger than the dimension of the space. In many cases however, a frame may reduce to a simple basis. The specific frames used in this work are not a basis since the frame elements are required to have the OSL property. The cost paid for using a frame which is not a basis is the numerical construction of the associated dual frame needed to complete the frame decomposition and reconstruction process. A frame representation for a waveform  $f$  is mathematically stated

$$\forall f \in \mathcal{H}, \quad f = \sum_n \tilde{\psi}_n \langle \psi_n, f \rangle \quad (1)$$

where  $\{\psi_n\}$  and  $\{\tilde{\psi}_n\}$  are the original and dual frames, respectively; and  $n \in J$ , a denumerable set. From frame theory, the dual frame elements are found from the operator equation

$$\tilde{\psi}_n = \frac{2}{A+B} \sum_{k=0}^{\infty} \left( 1 - \frac{2}{A+B} \sum_{n=-\infty}^{\infty} \psi_n \langle \psi_n, \cdot \rangle \right)^k \psi_n \quad (2)$$

where  $B \geq A > 0$ , are the frame bounds. If  $A = B$  the frame is said to be tight and the closer  $A$  is to  $B$ , the faster the convergence in (2). For both the Weyl-Heisenberg and the wavelet frames the snugness can be adjusted by oversampling, but the details are somewhat different. In this work four times oversampling is used with each type of frame resulting in extremely snug frames. A more detailed discussion is given in [1] where the frame bounds are computed for different cases. For the Weyl-Heisenberg case the frame elements are related by translation and modulation expressed as

$$g_{mn}(x) = g(x - nq_0) e^{im_p x}, \quad (3)$$

where to realize the OSL property, the Gaussian mother function

$$g(x) = \pi^{-\frac{1}{4}} e^{-\frac{x^2}{2}} \quad (4)$$

is used. For four times oversampling  $p_0 q_0 = \pi/2$ , and with  $q_0 = 1$  the frame bounds are  $A = 3.854$  and  $B = 4.147$  [1]. For the wavelet case the frame elements are related by translation and dilation expressed as

$$g_{mn}^{\pm}(x) = a_0^{-\frac{m}{2}} g(\pm a_0^{-m} x - nb_0) \quad (5)$$

where to realize the OSL property here, the modulated Gaussian mother function

$$g(x) = \pi^{-\frac{1}{4}} (e^{-ivx} - e^{-\frac{v^2}{2}}) e^{-\frac{x^2}{2}} \quad (6)$$

is used. The  $\pm$  sign in (5) designates the positive and negative frequency half spaces which must be handled separately [1,3], and  $\nu = \pi(2/\ln 2)^{0.5}$ . Oversampling in the Wavelet case is introduced in frequency only through dilation expressed as

$$g^\lambda(x) = a_0^{-\frac{\lambda}{N}} g(a_0^{-\frac{\lambda}{N}} x) \quad (7)$$

where  $\lambda = 0, \dots, N-1$  for  $N$  times oversampling. With  $N = 4$ ,  $a_0 = 2$ , and  $b_0 = 1$  the frame bounds are  $A = 6.918$  and  $B = 6.923$  [1]. To use (3) or (5) with (1) and (2) the number of summations are increased to account for the indices. The magnitude of the standard  $L^2(\mathbb{R})$  inner products  $\langle g_{mn}(x), f(x) \rangle$  given in (1) indicate the coupling of  $f(x)$  to the coherent states defined by  $\{g_{mn}\}$ , and the complete set represents a unique phase space signature. For each of the frames used here a range of  $(m, n)$  is selected to ensure reconstruction with negligible error when all the frame elements are used. The  $\{g_{mn}\}$  are projected onto the image azimuth cuts (direction of SAR formation) to represent the image in phase space. The filter responses are obtained by identifying coherent states with large information present and performing limited reconstruction. A minimum mean square error or percent power recovered at the filter output is used for the filter performance criteria. A filtered response is then obtained by limiting the reconstruction to dominant frame contributions.

### SAR Ocean Image Filtering

In this section frame filtering is performed on a SAR ocean image of a torn ship wake using both the Weyl-Heisenberg and Wavelet frames previously discussed. The image was provided by the Naval Air Warfare Center, Aircraft Division Warminster (NAWC/ADW) SAR image processing facility from experiments conducted off the east coast of the United States during the Fall of 1988. The image was formed from C-Band data collected at VV polarization and is shown in Figure 1. The dominant features represent a ship wake torn from conflicting velocity fields present on the ocean surface. The image size is (down range  $\times$  cross range) = (201  $\times$  402) pixels, and the pixel dimensions are (range, azimuth) = (2.5, 2.16) meters.

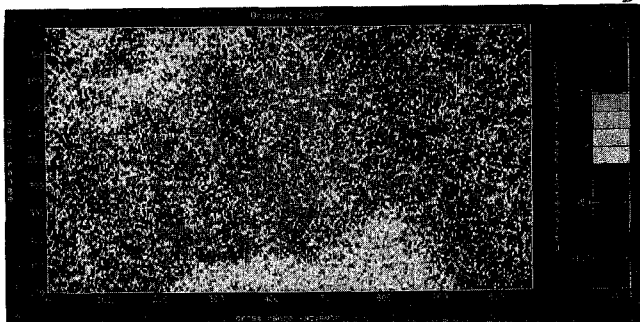


Figure 1: Original SAR image (C-Band VV polarization).

To first illustrate the filtering performance, consider the reconstructed azimuth cut shown in Figure 2 taken from the lower edge of the original image. Figure 2(a) shows both an almost perfect reconstruction by the dotted line, and a filtered cut superimposed by the solid line using the Weyl-Heisenberg frame. The almost perfect reconstruction uses 1,474 terms to recover 99% of the original power. The corresponding mean square error is approximately 0.06%. The filtered cut uses only 77 terms to provide 75% of the original power. Figure 2(b)-(c) shows the corresponding rate of power recovery and reduction in mean square error as a function of the number of terms used in the reconstruction. The dominant waveform feature efficiently preserved in the filtered response demonstrates the OSL property of the Weyl-Heisenberg frame used.

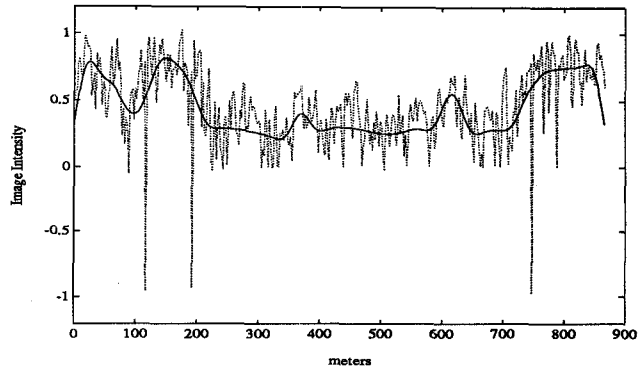


Figure 2(a): Original (dotted) and filtered (solid) azimuth cut (Weyl-Heisenberg case).

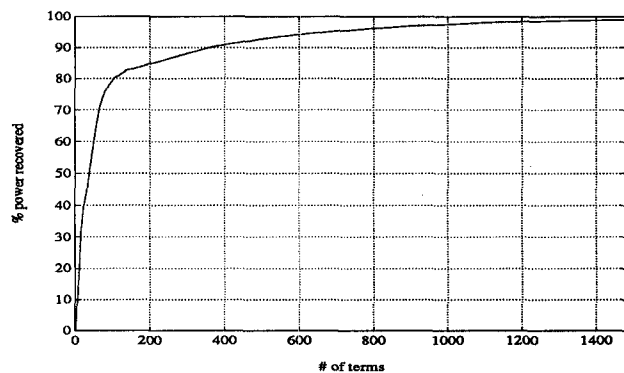


Figure 2(b): Filter recovered power efficiency (Weyl-Heisenberg case).

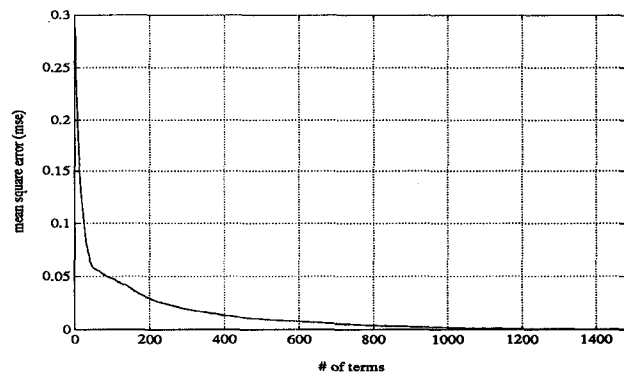


Figure 2(c): Mean square error at the filter output (Weyl-Heisenberg case).

Similar results are shown in Figure 3 using the wavelet frame. Here the almost perfect reconstruction uses 2,390 terms to recover 90% of the original power with corresponding mean square error of approximately 2.32%. The filtered cut uses 431 terms to recover 75%. Figure 3(b)-(c) shows the corresponding rate of power recovery and reduction in mean square error. As in the Weyl-Heisenberg case, the filtered response shows the efficient preservation of the waveform's dominant features resulting from the OSL property of the wavelet frame used. These examples illustrate the convergence properties of the filtering algorithm with both frames, and demonstrate the filter response is an approximation to its input.

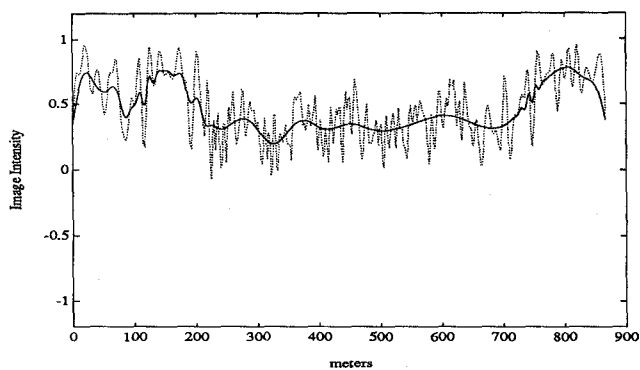


Figure 3(a): Original (dotted) and filtered (solid) azimuth cut (wavelet case).

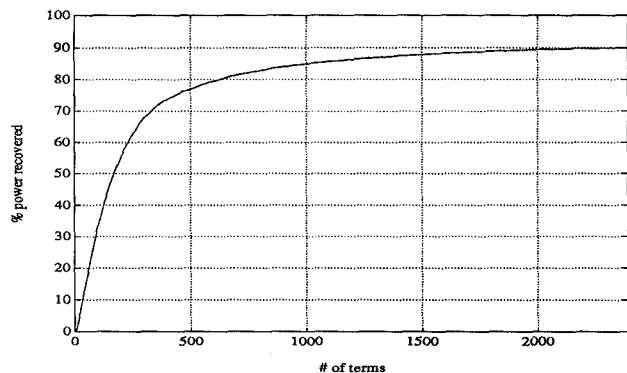


Figure 3(b): Filter recovered power efficiency (wavelet case).

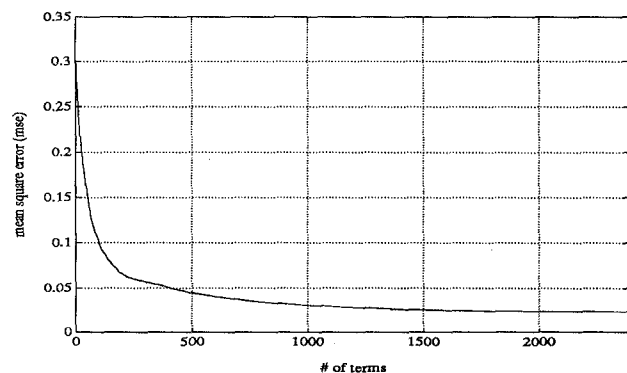


Figure 3(c): Mean square error at the filter output (wavelet case).

The filter algorithm can be applied to either one or both of the original image's linear dimensions. For the results shown here the filter is applied in the azimuth dimension. The results using the Weyl-Heisenberg frame are shown in Figure 4. It should be immediately apparent that the weak feature present in the original image is well maintained using far less data. Similarly, the results using the wavelet frame shown in Figure 5 demonstrate less data being needed to reasonably maintain the original feature information. For both results the power recovered is 50% of the original image of Figure 1. In the Weyl-Heisenberg case less than 10% of the data in the original image is used. The wavelet case uses less than 39% of the data in the original image, and although it requires more than the Weyl-Heisenberg case, it is still a significant reduction. The additional data arises from the difficulty that the wavelet analysis has in representing very low frequency information [3]. Note that from (6) it can be deduced that wavelet decompositions contain no terms that are DC-coupled (mapped precisely centered around zero frequency) which explains this difficulty.

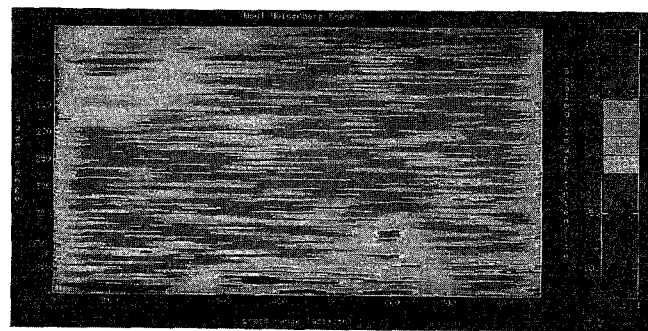


Figure 4: Filtered SAR image (Weyl-Heisenberg case).

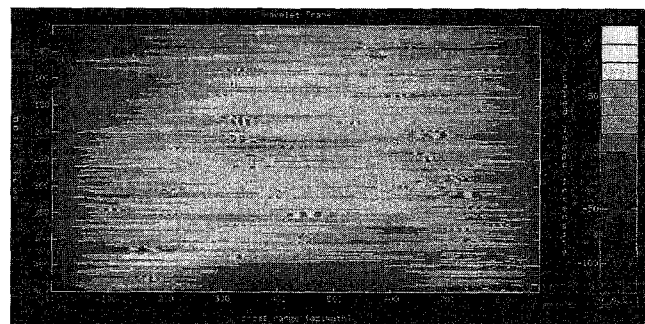


Figure 5: Filtered SAR image (wavelet case).

## Conclusions

The image information in azimuth (direction of SAR formation) is projected onto the discrete lattice locations in phase space with localization properties that meet the lower limit of the uncertainty principle. The filter responses are obtained by identifying lattice locations with large information present and performing a limited reconstruction. A minimum mean square error or percent power recovered at the filter output is used for the filter performance criteria. The procedure is both numerically tractable and stable once the dual frame in (2) has been constructed. The filtered image results in Figures 4 and 5 both represent a significant reduction in the data being required to retain the dominant image features. The two filtered images illustrate how the filter's response differs for each frame. The difference is a result of the particular frequency partitioning associated with the original image's representation on each frame. The filtered imagery shows that sharp edges are more efficiently represented on the wavelet frame, whereas the Weyl-Heisenberg frame is more efficient at representing slowly varying low frequency image features. Together, both types of frames when constructed to have the OSL property are felt not only to effectively remove speckle artifacts, but also to contain the necessary information for enhanced feature detection, extraction and identification.

## Acknowledgement

A sincere thanks is extended to Nicholas Tavani of the NAWC/ADW Daniel A. Rosso, Jr. Laboratory for his computer system support, and James Verdi, the P-3 SAR Program Director, for his interest and partial support of this work.

## References

- [1] I. Daubechies, "The Wavelet Transform, Time Frequency Localization and Signal Analysis," *IEEE Trans. on Information Theory*, vol. IT-36, no. 5, pp. 961-1005, Sept. 1990.
- [2] J. G. Teti, Jr. and H. N. Kritikos, "SAR Ocean Image Decomposition Using the Gabor Expansion," *IEEE Trans. on Geoscience and Remote Sensing*, vol. 30, no. 1, January, 1992.
- [3] J. G. Teti, Jr. and H. N. Kritikos, "SAR Ocean Image Representation Using Wavelets," submitted to *IEEE Trans. on Geoscience and Remote Sensing*, 1992.